Journal of Structural Biology 188 (2014) 259–266

Contents lists available at ScienceDirect

Journal of Structural Biology

journal homepage: www.elsevier.com/locate/yjsbi

Separation of replication and transcription domains in nucleoli

E. Smirnov [a,*], J. Borkovec [a], L. Kováčik [a], S. Svidenská [a], A. Schröfel [a], M. Skalníková [a], Z. Švindrych [a], P. Křížek [a], M. Ovesný [a], G.M. Hagen [a], P. Juda [a], K. Michalová [b], M.C. Cardoso [c], D. Cmarko [a], I. Raška [a]

[a] Institute of Cell Biology and Pathology, First Faculty of Medicine, Charles University in Prague, Prague, Czech Republic
[b] Centre of Oncocytogenetics, Institute of Medical Biochemistry and Laboratory Diagnosis, General University Hospital and First Faculty of Medicine, Charles University in Prague, Czech Republic
[c] Department of Biology, Technische Universitat Darmstadt, Darmstadt, Germany

ARTICLE INFO

Article history:
Received 29 April 2014
Received in revised form 2 October 2014
Accepted 5 October 2014
Available online 17 October 2014

Keywords:
Nucleolus
Replication
Transcription
rDNA
Super-resolution
Single-molecule localization microscopy

ABSTRACT

In mammalian cells, active ribosomal genes produce the 18S, 5.8S and 28S RNAs of ribosomal particles. Transcription levels of these genes are very high throughout interphase, and the cell needs a special strategy to avoid collision of the DNA polymerase and RNA polymerase machineries. To investigate this problem, we measured the correlation of various replication and transcription signals in the nucleoli of HeLa, HT-1080 and NIH 3T3 cells using a specially devised software for analysis of confocal images. Additionally, to follow the relationship between nucleolar replication and transcription in living cells, we produced a stable cell line expressing GFP-RPA43 (subunit of RNA polymerase I, pol I) and RFP-PCNA (the sliding clamp protein) based on human fibrosarcoma HT-1080 cells. We found that replication and transcription signals are more efficiently separated in nucleoli than in the nucleoplasm. In the course of S phase, separation of PCNA and pol I signals gradually increased. During the same period, separation of pol I and incorporated Cy5-dUTP signals decreased. Analysis of single molecule localization microscopy (SMLM) images indicated that transcriptionally active FC/DFC units (i.e. fibrillar centers with adjacent dense fibrillar components) did not incorporate DNA nucleotides. Taken together, our data show that replication of the ribosomal genes is spatially separated from their transcription, and FC/DFC units may provide a structural basis for that separation.

1. Introduction

Replication and transcription enzymatic complexes run at high speed and for long distances, which apparently compels the cell to employ a special strategy in order to prevent collision of the DNA and RNA polymerases. This need seems to be particularly urgent in the nucleoli, owing to certain aspects of their organization. In mammalian cells, nucleoli are formed on the basis of Nucleolus Organizer Regions (NORs), i.e. the clusters of ribosomal genes coding for 18S, 5.8S and 28S RNAs of the ribosomal particles (Henderson et al., 1972; Long and Dawid, 1980; Puvion-Dutilleul et al., 1991; Raška, 2003; Raška et al., 2006a,b; Cmarko et al., 2008; Sirri et al., 2008). When the cell enters S phase, the transcription activity of these genes continues and may even increase (Gorski et al., 2008). Moreover, replication of rDNA may be initiated in the transcribed as well as non-transcribed loci and proceed in both directions (Little et al., 1993; Yoon et al., 1995). Then how are the two machineries segregated?

So far this intriguing problem has not drawn special attention partly because of the specific structure of nucleoli in which individual rDNA repeats are "hidden" and the chief structural elements are represented by fibrillar centers (FCs), dense fibrillar components (DFCs), and granular components. All pol I dependent transcription in the nucleoli seems to take place in the DFC or in the border region between the DFC and the FC (e.g. Raška et al., 1983a,b, 1995, 2006a,b; Cmarko et al., 1999, 2000; Melčak et al., 1996; Malinský et al., 2002; Koberna et al., 2002; Casafont et al., 2006). As for rDNA replication, it is still not clear whether it occurs in the same regions as transcription. It has been established that the transcriptionally active genes, which in cycling cells represent about a half of the entire rDNA (Warner, 1999; Grummt and Pikaard, 2003), are replicated in early S phase, and replication of the silent genes is postponed until late S phase (Berger et al., 1997; Li et al., 2004), so that the problem of collision is chiefly confined to the early S phase. But there is yet another complication: trying to detect nucleolar replication *in situ* by incorporation of labeled nucleotides, one finds that the intensity of the signal is usually very low, especially in early S phase. The causes of this

* Corresponding author.

http://dx.doi.org/10.1016/j.jsb.2014.10.001
1047-8477/

phenomenon are not clear. According to one hypothesis (Dimitrova, 2011), rDNA may move to the nucleolar periphery, or even to the surrounding nucleoplasm, replicate there, and then pull back to its original position.

In the present work we focused on two aspects of the problem: (1) the spatial separation of replication and transcription foci in nucleoli; (2) relocation of nucleolar DNA in the course of S phase. To investigate these problems, we measured the spatial correlation of various replication and transcription signals in the nucleoli in cells of human and murine origin using specially devised software for analysis of confocal images. We also studied colocalization of replication and transcription foci employing a super-resolution single molecule localization microscopy (SMLM) method (Křížek et al., 2011; Ovesný et al., 2014). To observe the relocation of nucleolar DNA, we labeled it in early S phase with Cy5-dUTP in a cell line expressing RFP-PCNA and GFP-RPA43.

2. Methods

2.1. Cell culture and plasmids

Human derived HeLa and HT-1080 (human fibrosarcoma) cells were cultivated at 37 °C in Dulbecco modified Eagle's medium (DMEM, Sigma, #D5546) containing 10% fetal calf serum, 1% glutamine, 0.1% gentamycin, and 0.85 g/l $NaHCO_3$ in standard incubators. Mouse NIH 3T3 cells were maintained in DMEM supplemented with 10% calf serum and 1 mg/ml penicillin/streptomycin.

We produced a cell line stably expressing two plasmid constructs: RFP-PCNA vector was received from the Max Planck Institute for Molecular Cell Biology and Genetics, Dresden; and GFP-RPA43 vector was received from Laboratory of Receptor Biology and Gene Expression Bethesda, MD (Dunder et al., 2002). Both constructs were transfected into the HT-1080 cells using Fugene (Qiagen) and stable clones were selected with G418 (GIBCO). One clone with bright two-colored fluorescence was chosen and expanded into the cell line.

2.2. Incorporation of DNA and RNA nucleotides

For simultaneous labeling of replication and transcription sites, sub-confluent cells were incubated 5 min with a mixture of 5-ethynyl-2′-deoxyuridine (EdU) (Invitrogen) at a concentration of 10 μM, and 5-fluorouridine (FU) (Sigma) at a concentration of 10 μM.

The cells were fixed in 2% formaldehyde freshly prepared from paraformaldehyde, permeabilized with Triton X-100, and processed for FU immunocytochemistry using a mouse monoclonal anti-BrdU antibody (Sigma). After that the replication signal was visualized using EdU Alexa Fluor 647 Imaging Kit (Invitrogen). Additionally, we visualized the replication signal using Cy3-dUTP and Cy5-dUTP using the scratch procedure (Schermelleh et al., 2001).

2.3. Immunocytochemistry

Primary antibodies against human rRNA polymerase (pol I) and Upstream Binding Factor (UBF) were kindly provided by Dr. U. Scheer (Biocenter of the University of Wurzburg). We also used a monoclonal (mouse) anti-UBF antibody (Santa Cruz Biotechnology, Inc.).

For visualization of fibrillarin in nucleoli, we used monoclonal antibodies against human fibrillarin or mouse fibrillarin (clone 17C12), kindly donated by Kenneth M. Pollard (Scripps Research Institute, La Jolla, CA). Secondary anti-human and anti-mouse antibodies were conjugated with Alexa 532 (Invitrogen), Cy3, or DyLight 488 (both from Jackson ImmunoResearch Laboratories). Coverslips with the cells were then mounted in Mowiol and allowed to harden overnight before imaging.

2.4. Microscopy

Confocal images were acquired using a SP5 (Leica) confocal laser scanning microscope equipped with a 63×/1.4NA oil immersion objective. Live cell imaging was performed with a spinning disk confocal system based on an Olympus IX81 microscope equipped with an Olympus UPlanSApo 100×/1.4NA oil immersion objective, CSU-X spinning disk module (Yokogawa) and Ixon Ultra EMCCD camera (Andor). For live cell imaging cells were maintained at 37 °C and 5% CO_2 using a microscope incubator (Okolab). For live cell microscopy, cells were cultured in glass bottom Petri dishes (MatTek).

For single molecule localization microscopy, we used an Olympus IX70 microscope equipped with an Olympus planapochromatic 100×/1.45NA oil immersion objective and a front-illuminated EMCCD camera (Ixon DU885, Andor). The back-projected pixel size in the sample was 80 nm. For imaging of Alexa 647 labeled EdU, we used a 630 nm, 500 mW diode laser, while for imaging of Alexa 532 labeled fluorouridine, we used a 532 nm, 1000 mW DPSS laser (both from Dragon laser, ChangChun, China). The laser light was delivered to the microscope using a multimode optical fiber (M29L02, Thor Labs) and a custom-made critical illumination setup which imaged the end face of the fiber into the sample. Power densities at the sample for both lasers were approximately 2 kW/cm^2. Fluorescence was isolated using a custom dual band filter set for SMLM (emission bands 569–610 nm and 667–736 nm, Chroma).

2.5. Software and data analysis

For colocalization analysis of the confocal image stacks, we developed a custom ImageJ plugin (available at https://github.com/vmodrosedem/segmentation-correlation). Using images from both channels, the program identifies the regions occupied by nucleoli and calculates Pearson's correlation coefficient (PCC) and Spearman's rank coefficient (SRC) between the signals corresponding to the two channels within the volume of nucleoli. Additionally, the program measures the areas (in pixels) occupied by the nucleoli and the average intensities of both signals within these areas.

To achieve this, the software first identifies areas with nuclei (in cells positive for EDU replication signals) by creating a maximum intensity projection of the confocal image stack, then blurring the projection with a Gaussian filter (σ = 8–10 pixels), and finally thresholding the blurred image with a value obtained by Otsu's method for automatic threshold selection. The obtained mask of segmented nuclei is subjected to a hole filling operation using a binary, 4-way recursive flood fill algorithm. If several nuclei are found in a single image, they are identified by labeling of connected components. To segment nucleoli within each nucleus, we blurred each 2D confocal image (FU signal) with a Gaussian filter (σ = 3 pixels), followed by automatic threshold selection using Otsu's method. Regions with an area smaller than a user-specified value (300–400 pixels) were discarded to ignore nucleoplasmic signals. The two channels and their respective masks were then combined to identify nucleoli within each nucleus. All images were inspected visually to ensure that the segmentation was accurate. The calculation of PCC and SRC between the signals was limited to the intersection of the nuclear and nucleolar masks and was performed on the raw data without any background subtraction or normalization.

For SMLM data processing, we used ThunderSTORM (Ovesný et al., 2014), an open-source plugin for ImageJ designed for

comprehensive analysis of single-molecule super-resolution data. Briefly, the settings were as follows. For approximate localization of molecules, we used a wavelet-based image filter followed by local intensity maximum detection. To localize molecules with sub-pixel precision, we used a maximum likelihood fitting approach with a Gaussian point spread function model. We then corrected the data for a sample drift using a cross-correlation method, and removed molecules with poor localization parameters. Molecules localized within a 30 nm radius that were detected in subsequent frames were merged into a single localization. Super-resolution images were visualized using a method based on average shifted histograms (for more details, see Ovesný et al., 2014).

Cross-correlation of thresholded images as described above is a suitable method for colocalization analysis of intensity-based data (e.g. confocal images). In SMLM, the super-resolution data is represented as a list of coordinates of individual molecules, so approaches based on intermolecular distances may be exploited. To evaluate colocalization in SMLM experiments, we randomly selected four 1 μm^2 regions within the nucleoli and calculated histograms of pair-wise distances between the two channels (Alexa 647-labeled EdU and Alexa 532-labeled FU or Alexa 532-labeled fibrillarin). The histograms were normalized to account for the effect of increased numbers of pairs at larger distances by dividing the count in each bin by its corresponding distance.

3. Results

3.1. Negative correlation of the replication and transcription signals in nucleoli

To label replication and transcription sites in HeLa, HT 1080, and NIH 3T3 cells, we incubated these cells with a mixture of 5-ethynyl-2′-deoxyuridine (EdU) and 5-fluorouridine (FU) for 5 min. Stacks of confocal sections (Fig. 1A and B) were analysed by the specially devised program (see Methods) which defined the regions occupied by the nucleoli. Within these regions, the program measured the PCC and SRC between the intensities of replication and transcription signals (Fig. 1C and D). In all three cell lines, both correlation coefficients usually took negative values within nucleoli, and PCC never differed significantly from SRC (data shown only for HeLa cells).

Measuring PCC between replication and transcription signals locally within the cell nuclei (Fig. 1C and D), we found that the correlation was usually negative in the nucleoli, but positive in the nucleoplasm. In background regions outside the cell nucleus, PCC was close to zero, but usually positive. Similar differences between nucleoli and nucleoplasm were observed when, instead of FU, we used pol I or UBF immunocytochemical signals (data not shown). These differences apparently refer to a special property of nucleoli rather than to a peculiarity of a certain staining method.

To assess the capacity of the analysis program, we applied it to images in which the value of PCC was expected to be positive or negative *a priori* (Fig. 2). In these experiments, correlation of two replication signals (simultaneously incorporated EdU and Cy3dUTP) took highly positive values (PCC = 0.86, Fig. 2A). Correlation between immunocytochemically detected UBF and EdU signals, measured in the whole cell nucleus in early S phase, was negative (PCC = −0.72, Fig. 2B).

To examine influence of the intensity of fluorescence signals upon correlation between their intensities, we measured PCC on the same cell at different confocal laser powers (Fig. 2C and D). In all the studied cases, the value of correlation was little changed with respect to the recorded signal intensities.

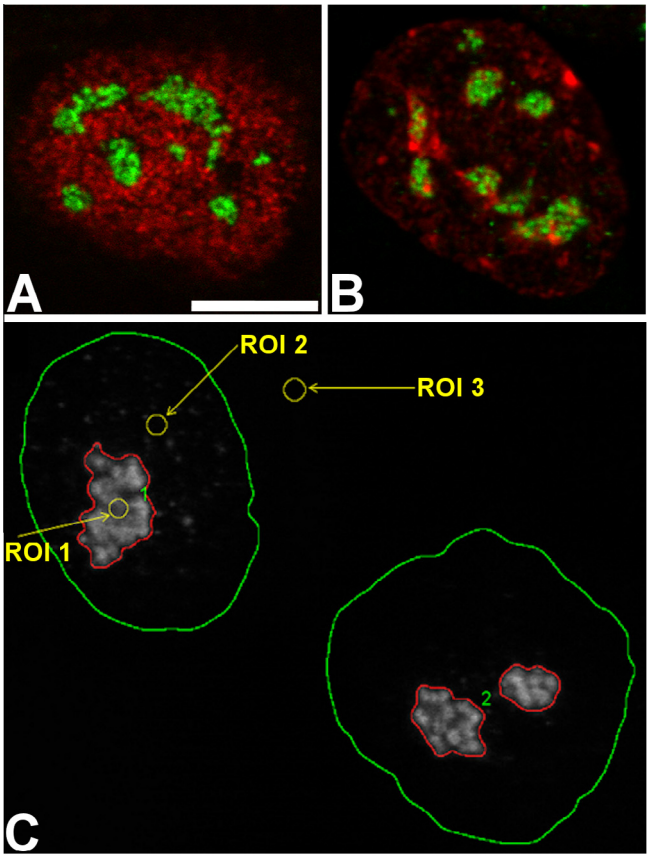

Cell #	PCC	SRC	rand. PCC	area	$\bar{I}_1$	$\bar{I}_2$
1	-0,38	-0,38	1,9e-3	73941	5953	11160
2	-0,32	-0,29	-9,0e-4	63803	4775	11005

ROI 1: -0,30 **ROI 2:** +0,28 **ROI 3:** +0,01

D

Fig.1. Application of the program for measuring correlation (PCC and SRC) between replication and transcription signals in nucleoli in confocal images of HeLa cells. (A and B) Confocal sections of the replication (EdU, red) and transcription (FU, green) signals in HeLa cells, representing examples of early S phase (A) and late S phase (B). The FU signal in the nucleoli has a grainy structure in which single grains apparently correspond to FC/DFC units. Scale bar: 5 μm. (C and D) Application of the program in two cells. (C) One optical section with outlines of the nuclei (green) and nucleoli (red). Three regions of interest (ROIs) are indicated by arrows. (D) data from measurements for the two cells and three ROIs. $\bar{I}_1, \bar{I}_2$ represent the average intensities of EdU and FU signals within the nucleoli. The values of PCC and SRC are negative in the nucleoli (ROI 1), positive in the nucleoplasm (ROI 2), close to 0 in the background (ROI 3).

Since the Pearson's correlation between the signals of replication and transcription in the nucleoli was negative, we used the modulus of this correlation coefficient (MC). We followed the dynamics of this value in the course of S phase, which we divide into four stages, S1–4, based upon the distinct morphological criteria (Smirnov et al., 2011). In this scheme, S1 corresponds to early S phase, when numerous replication foci are evenly distributed in the nucleoplasm. In S3, which is often called mid S phase, there are typical fringes of coarse replication foci along the lamina and around the nucleoli, in the nucleoplasm the foci are large and surrounded by vast spaces. S2 is the intermediate stage in which the foci are fine and numerous, but the sublaminar fringes can be already distinguished. Stage S4 is the very end of S phase; replication foci are large and sparse, distributed without any particular pattern, and altogether occupy a small part of the nucleus. All these

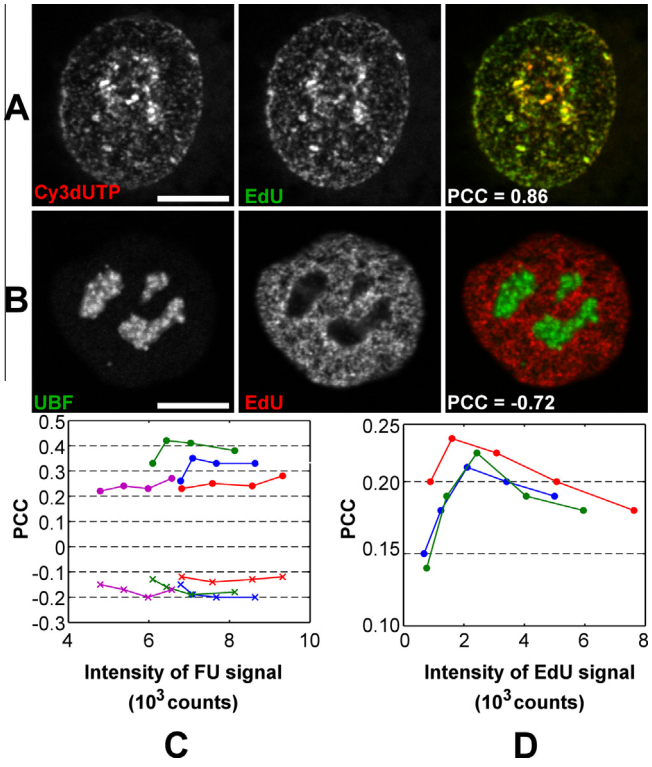

Fig.2. Testing of the program for measuring correlation in HeLa cells. (A) Simultaneous incorporation of Cy3dUTP (red) and EdU (green). The signals are well colocalized; PCC measured in the whole cell nucleus is +0.86. (B) Immunostaining of UBF (green) and EdU (red). The signals are largely anti-colocalized; PCC measured in the whole nucleus is −0.72. (C and D) PCC measured in the same cells with variable intensity of the transcription (C, four cells), or replication (D, three cells) signals, achieved by varying the power of the lasers in the confocal microscope. Data on each cell are represented by a particular color. In the nucleoplasm (circles), the values of PCC remain positive; in the nucleoli (crosses), they are negative. Scale bars: 5 μm.

patterns are formed by replication foci approximately 120 nm in size that are stably maintained throughout the cell cycle (Koberna et al., 2005; Baddeley et al., 2009; Casas-Delucchi and Cardoso, 2011; Reinhart et al., 2013).

We found that the value of MC significantly increased from S1 to S3 (from 0.23 to 0.31, Table 1). From S3 to S4 there was no significant change (data not shown). In pulse-chase experiments, when FU was incorporated after a 3 h pulse of EdU, MC was reduced to 0.13 from 0.23 (Table 1). Remarkably, whereas local intensities of replication and transcription signals correlated negatively, the integral intensity of transcription signals (measured in whole nucleoli) positively correlated with the integral intensity of nucleolar replication; at stage S1, the linear correlation of these

Table 1
Values of spatial correlation (PCC and SRC) between the intensities of EdU and FU signals (EdU/FU), and between Fibrillarin and EdU (EdU/fibrillarin) signals in the nucleoli. The values were measured in fixed HeLa cells. In the control (ctrl), EdU was added to the cells together with FU for 5 min before fixation. In the pulse-chase experiments, the cells were fixed 3 h after a 5 min pulse of EdU.

	EdU/FU		EdU/fibrillarin
	PCC ± Std.	SRC ± Std.	PCC ± Std.
S1, ctrl	−0.23 ± 0.02	−0.21 ± 0.02	−0.28 ± 0.01
S3, ctrl	−0.31 ± 0.02	−0.32 ± 0.02	−0.28 ± 0.01
S1, chase 3 h	−0.13 ± 0.02	−0.11 ± 0.02	−0.27 ± 0.01
S3, chase 3 h	−0.28 ± 0.03	−0.25 ± 0.02	

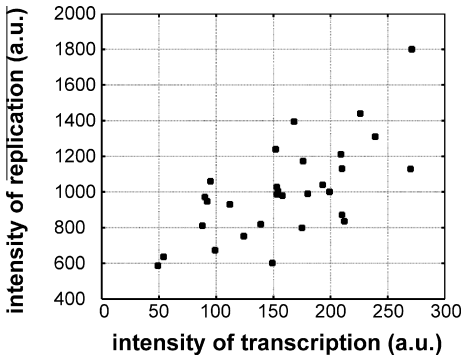

Fig.3. Cell-by-cell measurements of the relationship between the average intensities of replication and transcription signals in the nucleoli of HeLa cells in phase S1. Intensities of both signals were measured in 30 cells. $R = 0.67$.

two intensities was $r = 0.67$ (Fig. 3). This circumstance seems to reflect the efficiency of the separation of the two signals.

PCC between the signals of replication (EdU) and fibrillarin in nucleoli also proved to be negative (Table 1). But in pulse-chase experiments, when the cells were fixed and stained for fibrillarin after a 3 h pulse of EdU, we found no significant difference between the values obtained in the experiment and in the control (Table 1). These data indicate that the distribution of fibrillarin in the nucleoli is not significantly influenced by the progress of replication.

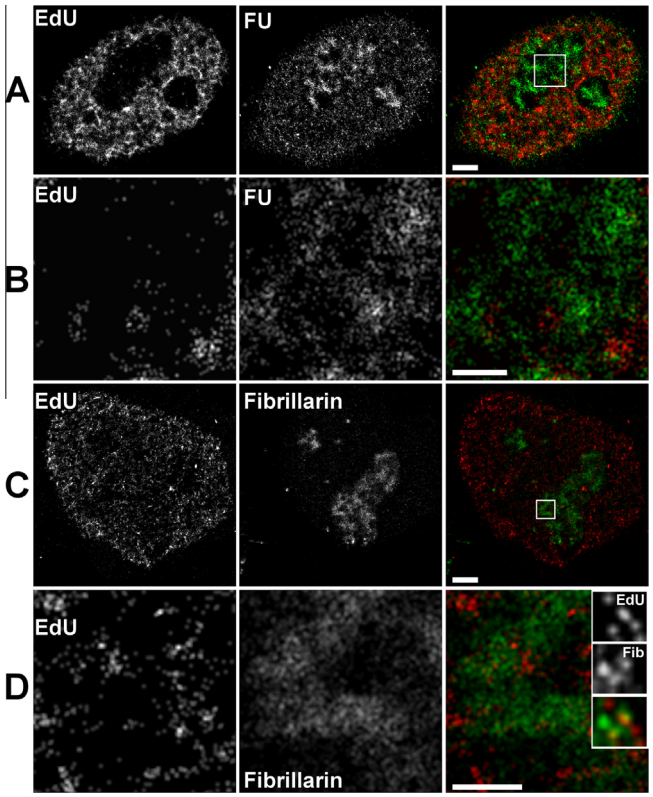

Fig.4. Super-resolution (SMLM) images (A) replication (EdU, red) and transcription (FU, green) signals in phase S1. Scale bar: 1 μm. (B) An area within nucleolus, showing little or no colocalization of EdU and FU signals. Scale bar: 0.3 μm. (C) Replication (EdU, red) and fibrillarin (green) in phase S1. Scale bar: 1 μm. (D) Detail of nucleolus, showing colocalization of EdU and fibrillarin. Scale bar: 0.3 μm. Inset: magnified area from D with colocalized foci.

3.2. Replication and transcription signals do not colocalize in single-molecule microscopy super-resolution images

In reconstructed SMLM images of replication and transcription signals (incorporation of EdU and FU, respectively) in HeLa cells at stage S1, we observed very few EdU and FU molecules in close proximity to each other within nucleoli (Fig. 4A and B). Apparently, there was no significant activity of DNA polymerase in the FC/DFC units engaged in rDNA transcription. In contrast, in super-resolution SMLM images representing EdU and immunostaining for fibrillarin, which is a component of DFCs, we detected several fibrillarin molecules at close distances (<200 nm) to EdU molecules (Fig. 4C and D).

To investigate these visual observations further, we constructed histograms of pair-wise distances between the detected EdU and FU molecules, and between EdU and fibrillarin molecules. In these histograms, we observed larger numbers of pairs of EdU and fibrillarin molecules at distances below ~200 nm than for EdU-FU pairs (Fig. 5). This distance scale is inaccessible to conventional confocal microscopy, however the findings are consistent with the results from colocalization analysis of confocal images of similarly prepared cells as described above and may suggest that rDNA transcription is arrested in the FC/DFC units involved in replication.

3.3. Separation of replication and transcription signals observed in living cells

For this part of the study we produced a stable HT 1080 cell line expressing RFP-PCNA and GFP-RPA43 (a subunit of RNA pol I). To test this cell line we introduced Cy5-dUTP following the scratch procedure (Schermelleh et al., 2001). In separate assays we added EDU and FU to the culture medium, fixed the cells, then processed them for immunostaining and the click chemistry-based EdU reaction. The results of these experiments are shown in Fig. 6. We found that RFP-PCNA and Cy5-dUTP signals colocalize, representing the replication foci (Fig. 6A); GFP-RPA43 and FU signals also colocalize, apparently labeling the FC/DFC units (Fig. 6B). In addition, MC for RFP-PCNA and GFP-RPA43 in the nucleoli strongly correlates with MC for EdU and GFP-RPA43 (Fig. 6C), as well as with MC for RFP-PCNA and FU (Fig. 6D). These results show that the examined cell line may be employed in the study of separation of the replication and transcription signals in nucleoli.

Using a spinning disk microscope, we recorded 3D stacks of individual cells expressing RFP-PCNA and GFP-RPA43 for 8 h periods to observe the transitions between G1, S, and G2 phases. The pattern of PCNA expression allowed us to determine which stage of S phase the cells were in. RPA43 signals were used for defining the nucleolar areas of the cells. To assess the progress of replication, another marker of DNA synthesis, Cy5-dUTP, was added to the cells at the beginning of the experiment. Observing stacks of confocal images in the three channels (Fig. 6E), we could follow the dynamics of the MC values in the couples GFP-RPA43/RFP-PCNA and GFP-RPA43/Cy5-dUTP measured in the same nucleoli. Our analysis indicates that MC for PCNA and RPA43 signals in the transfected cells increased between S1 and S3 stages of the S phase (Fig. 7A, black bars); during the same period MC for Cy5-dUTP and RPA43 decreased (Fig. 7A, white bars). These changes were gradual,

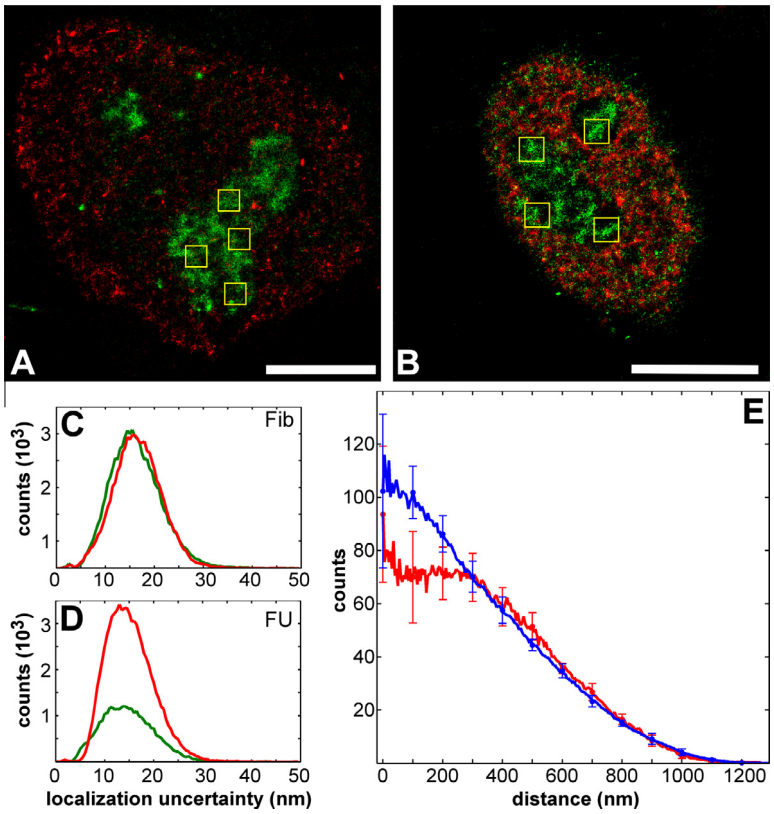

Fig.5. Analysis of colocalization in SMLM experiments (see Fig. 4). (A) EdU (red; 62,000 localizations) and fibrillarin (green; 68,000 localizations), (B) EdU (red; 180,000 localizations) and FU (green; 63,000 localizations). Scale bars: 5 μm. (C and D) Histograms of localization precision of the two experiments. In red – EdU, in green – fibrillarin (C) or FU (D). The mean values of the localization precision: 15.2 nm for FU; 16.6 nm for fibrillarin. (E) Normalized histogram of the pair-wise distances calculated from the four square regions (1×1 μm^2) indicated in A and B. The distribution of distances for the FU/EdU pairs and the Fibrillarin/EdU pairs differs within about 300 nm, which shows that the replication signal (EdU) tends to localize closer to Fibrillarin than to FU signals.

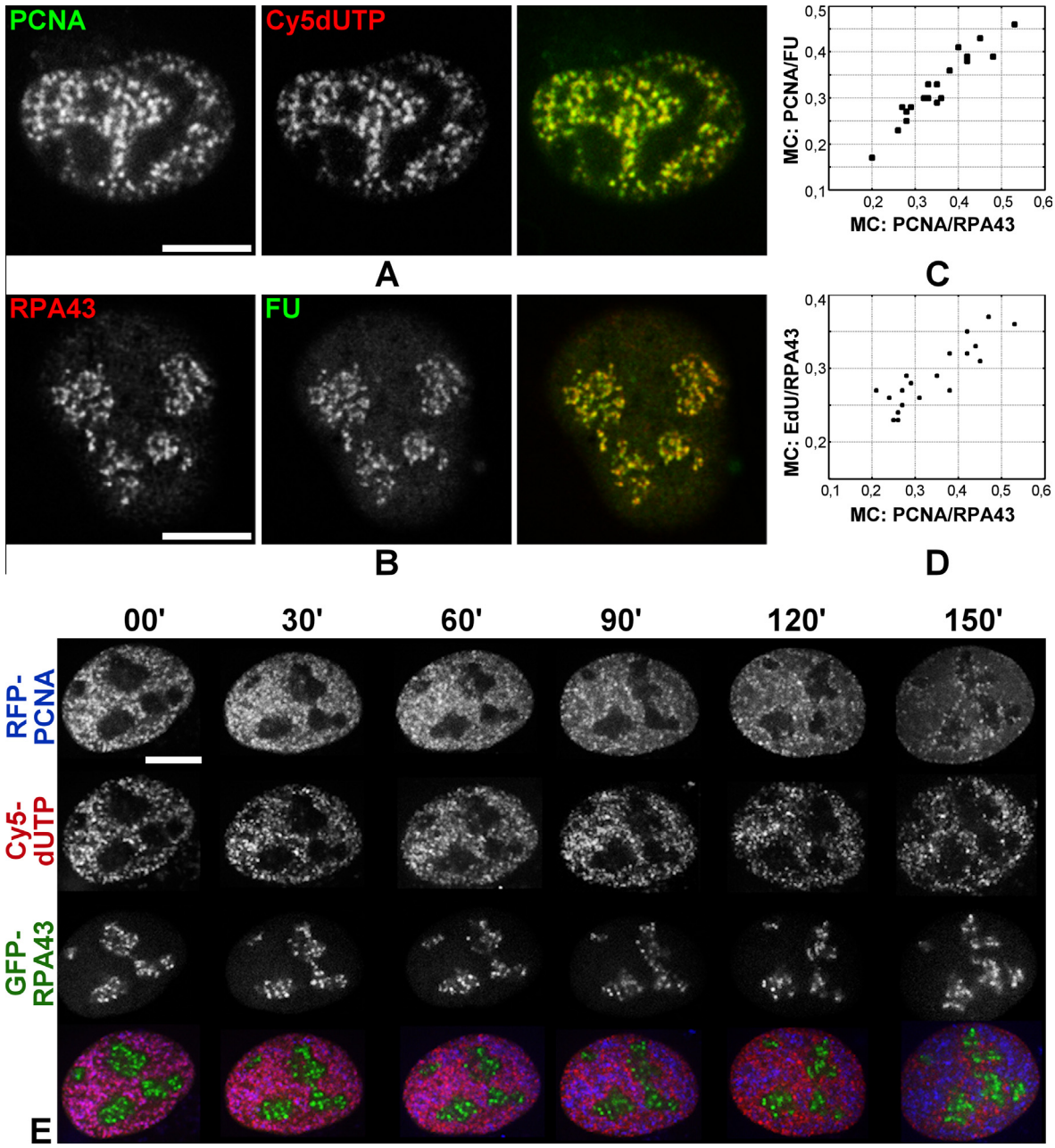

Fig.6. Dynamics of replication and transcription signals in a stable cell line expressing GFP-RPA43 and RFP-PCNA. RFP-PCNA marks replication foci. GFP-RPA43 marks active FC/DFC units of the nucleoli. (A) Colocalization of RFP-PCNA (green) and replication (pulse of Cy5-dUTP, red) signals in S1 phase. (B) Colocalization of GFP-RPA43 (red) and transcription (FU, green) signals in S1 phase. (C) The absolute value of the PCC (modulus of correlation, MC) of RFP-PCNA and GFP-RPA43 signals correlates with MC of RFP-PCNA and FU signals. (D) MC of RFP-PCNA and GFP-RPA43 signals correlates with MC of EdU and GFP-RPA43. (E) Following GFP-RPA43 (green), RFP-PCNA (red), and Cy5-dUTP (blue) in a living cell throughout S phase. The pattern of RFP-PCNA signal gradually changed from S1 (00 min) to S4 (150 min). The pattern of Cy5-dUTP signal does not change significantly in the course of S phase. Scale bars: 5 μm.

according to the results of the measurements in individual cells imaged at 1 h intervals (Fig. 7B).

3.4. Distribution of nucleolar DNA in the course of S phase

We followed the changes in the distribution of nucleolar DNA in live transfected cells that were additionally labeled with Cy5dUTP. Over the course of S phase, the shape of nucleoli and the distribution of signals within them continually changed (Fig. 8A and B). Nevertheless, in these experiments we observed no significant increase in Cy5dUTP labeling. In fact the intensity of the signal rather decreased as a result of photobleaching. For a quantitative assessment of the DNA exchange between the nucleoli and nucleoplasm, we measured the relative intensity of Cy5dUTP signals (namely, the intensity of this signal in nucleoli normalized by its intensity in the nucleoplasm). Selecting cells which incorporated Cy5dUTP at stage S1, we found that the results of the measurements did not change significantly from early S to G2 phase (Fig. 8D). In contrast, the relative intensity of PCNA-RFP in the same nucleoli sharply increased between S1 and S3 (Fig. 8C). To study the period from G1 to S1, we introduced Cy5dUTP to cells in early S phase, followed them through mitosis, and made

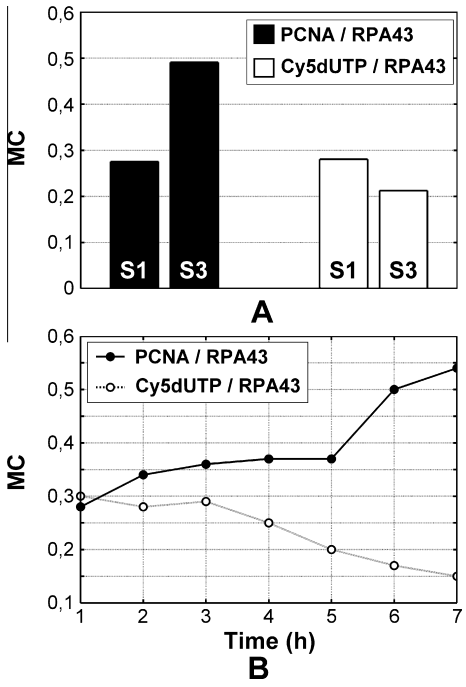

Fig.7. Dynamics of the MC of replication and transcription signals. From S1 to S3, MC of RFP-PCNA and GFP-RPA43 signals increases; MC of Cy5-dUTP and GFP-RPA43 decreases. These changes are gradual. (A) MC of RFP-PCNA and GFP-RPA43 signals (black bars), and Cy5-dUTP and GFP-RPA43 signals (white bars) measured in fixed cells. The differences between S1 and S3 are statistically significant ($P > 0.95$). (B) MC of Cy5-dUTP and GFP-RPA43 signals (white dots) and RFP-PCNA and GFP-RPA43 signals (black dots) in living cells during S phase. The two graphs represent measurement in the same cell (see discussion).

measurements on the daughter cells as they passed from G1 stage (they preserved the pattern of the stage S1 in which they had been labeled) to S1. Again, we found no significant change in the relative intensity of the signal (Fig. 8E). Therefore, in our cells there was no considerable exchange of DNA between nucleoli and nucleoplasm, at least from late G1 to early G2 phase of cell cycle.

4. Discussion

In mammalian cells rDNA replication occupies the entire S phase, apparently because a portion of ribosomal genes remain transcriptionally silent throughout interphase (Berger et al., 1997; Warner, 1999; Grummt and Pikaard, 2003; Li et al., 2004). At the beginning of S phase the nucleoplasmic chromatin seems to be segregated into zones (each containing about 1 Mb DNA) engaged in the synthesis of either RNA or DNA; the collision of different machineries can be thus partly avoided (Jackson and Pombo, 1998; Berezney et al., 2000; Koberna et al., 2005). Results of an EM study indicated that similar segregation may also be the case in nucleoli (Pliss et al., 2005), although the authors of this work did not show simultaneous labeling of replication and transcription signals in the same cell.

According to our light microscopic data (Fig. 1 and Table 1) the correlation between replication and transcription signals is usually negative in the nucleoli, but positive in the nucleoplasm. This indicates that replication and transcription machineries are separated in the nucleoli more efficiently than in the nucleoplasm.

The super-resolution microscopy data on replication and transcription foci (Fig. 4) suggest that FC/DFC units of nucleoli provide the structural basis for this effective separation, since active ribosomal genes belonging to different units are structurally isolated from one another. We suppose that each unit may accommodate either transcription or replication, but not both of these processes simultaneously. Indeed, when FU and EdU are administered to the cells simultaneously, the replication signal appears in FU-negative foci. On the other hand, incorporated EdU sometimes colocalizes with fibrillarin-positive foci. Since fibrillarin is a component of DFCs (Ochs et al., 1985; Scheer and Benavente, 1990), we suppose that replication occurs only in those FC/DFC units where

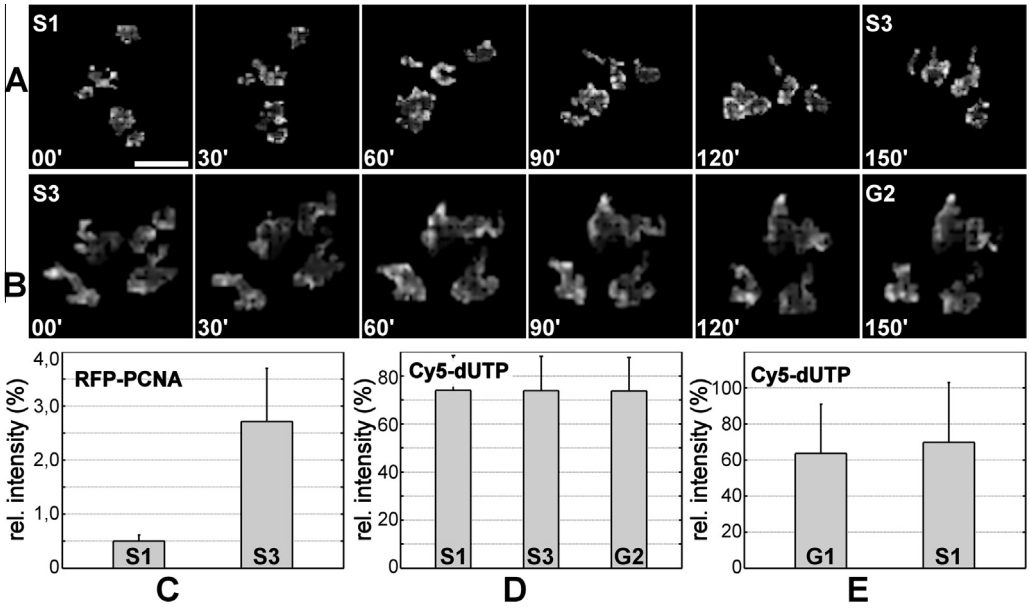

Fig.8. Following Cy5-dUTP signals within nucleoli during the course of the cell cycle in live cells. (A) Labeled DNA during the transition from S1 to S3. (B) Labeled DNA at the transition from S3 to G2. Since Cy5dUTP signals in the nucleoli were much weaker than in the nucleoplasm, we cropped the nucleolar regions in (A) and (B) and increased the brightness of the replication signal (Thus processed images were not used for subsequent measurements). Scale bar: 5 μm. (C) Relative intensity of RFP-PCNA signals (the intensity of the signal in the nucleoli normalized by its intensity in the nucleoplasm) in phases S1 and S3. (D) Relative intensity of Cy5-dUTP incorporated in S1 phase and then measured in S1, S3 and G2 phases. (E) Relative intensity of Cy5-dUTP incorporated in S1 phase and then measured in G1 and S1 phases of the next cell cycle (i.e., in the daughter cells). The data in (D) and (E) show no considerable exchange of DNA between nucleoli and nucleoplasm from G1 to G2, although the distribution of the labeled DNA within the nucleoli changes, as seen in (A) and (B).

transcription is suspended. This supposition agrees with our data about the dynamics of the separation (MC values) in the course of S phase (Fig. 7). In the first case, firing of the new replication forks is accompanied by the suspension of rDNA transcription in the respective FC/DFC units, while those units in which replication is finished become transcriptionally active again, thus the separation of the replication and transcription signals gradually increases. In the second case, replication signal (Cy5dUTP) incorporated in DNA remains in those units where transcription has resumed, and as the number of such units grows, the MC of the Cy5dUTP and transcription signals is decreasing.

According to our hypothesis, FC/DFC units are never shared by active pol I and DNA polymerase machineries. Nevertheless, this does not exclude a possibility of relocation of the transcriptionally active and/or silent nucleolar DNA in connection to its replication. In our observations on the dynamics of the replication signal *in vivo* from late G1 to early G2 phases of the cell cycle (Fig. 8), there was no significant exchange of DNA between nucleoli and nucleoplasm. Such exchange, if it takes place at all, cannot account for the low intensity of replication signal in the early S phase. Thus our results do not confirm the conjecture made by Dimitrova (2011) that relocation of rDNA may account for low intensity of replication signal in the nucleoli in early S phase. Nevertheless, the distribution of DNA within the nucleoli seems to change significantly, as the nucleoli grow and change their shape.

Taken together, our data show that in each moment of S phase, replication of the ribosomal genes is spatially separated from their transcription. This separation is probably achieved by suspension of the transcription in FC/DFC units which contain replicating DNA.

Acknowledgments

This work was supported by the Grant Agency of Czech Republic (P302/12/1885, 13-12317J, P302/12/G157), by Charles University in Prague (PRVOUK P27/LF1/1 and UNCE 204022), by OPPK (CZ.2.16/3.1.00/24010), by OPVK (CZ.1.07/2.3.00/30.0030), and by DFG (German Research Council) grant CA 198/9-1.

References

Baddeley, D., Chagin, V.O., Schermelleh, L., Martin, S., Pombo, A., Carlton, P.M., Gahl, A., Domaing, P., Birk, U., Leonhardt, H., Cremer, C., Cardoso, M.C., 2009. Measurement of replication structures at the nanometer scale using super-resolution light microscopy. Nucleic Acids Res. 38 (2), 1–11.

Berezney, R., Dubey, D.D., Huberman, J.A., 2000. Heterogeneity of eukaryotic replicons, replicon clusters, and replication foci. Chromosoma 108, 471–484.

Berger, C., Horlebein, A., Gogel, E., Grummt, F., 1997. Temporal order of replication of mouse ribosomal RNA genes during the cell cycle. Chromosoma 106, 479–484.

Casafont, I., Navascues, J., Pena, E., Lafarga, M., Berciano, M.T., 2006. Nuclear organization and dynamics of transcription sites in rat sensory ganglia neurons detected by incorporation of 5′-fluorouridine into nascent RNA. Neuroscience 14, 453–462.

Casas-Delucchi, C.S., Cardoso, M.C., 2011. Epigenetic control of DNA replication dynamics in mammals. Nucleus 5, 370–382.

Cmarko, D., Verschure, P.J., Martin, T.E., Dahmus, M.E., Krause, S., Fu, X.D., van Driel, R., Fakan, S., 1999. Ultrastructural analysis of transcription and splicing in the cell nucleus after bromo-UTP microinjection. Mol. Biol. Cell 10 (1), 211–223.

Cmarko, D., Verschure, P.J., Rothblum, L.I., Hernandez-Verdun, D., Amalric, F., van Driel, R., Fakan, S., 2000. Ultrastructural analysis of nucleolar transcription in cells microinjected with 5-bromo-UTP. Histochem. Cell Biol. 113, 181–187.

Cmarko, D., Smigova, J., Minichova, L., Popov, A., 2008. Nucleolus: the ribosome factory. Histol. Histopathol. 23 (10), 1291–1298.

Dimitrova, D.S., 2011. DNA replication initiation patterns and spatial dynamics of the human ribosomal RNA gene loci. J. Cell Sci. 124 (Pt 16), 2743–2752.

Dundr, M., Hoffmann-Rohrer, U., Hu, Q., Grummt, I., Rothblum, L.I., Phair, R.D., Misteli, T., 2002. A kinetic framework for a mammalian RNA polymerase in vivo. Science 298 (5598), 1623–1626.

Gorski, S.A., Snyder, S.K., John, S., Grummt, I., Misteli, T., 2008. Modulation of RNA polymerase assembly dynamics in transcriptional regulation. Mol. Cell 30 (4), 486–497.

Grummt, I., Pikaard, C.S., 2003. Epigenetic silencing of RNA polymerase I transcription. Nat. Rev. Mol. Cell Biol. 4, 641–649.

Henderson, A.S., Warburton, D., Atwood, K.C., 1972. Location of ribosomal DNA in the human chromosome complement. Proc. Natl. Acad. Sci. U.S.A. 69, 3394–3398.

Jackson, D.A., Pombo, A., 1998. Replicon clusters are stable units of chromosome structure: evidence that nuclear organization contributes to the efficient activation and propagation of S phase in human cells. J. Cell Biol. 140 (6), 1285–1295.

Koberna, K., Malínský, J., Pliss, A., Mavata, M., Vecerova, J., Fialová, M., Bednár, J., Raška, I., 2002. Ribosomal genes in focus: new transcripts label the dense fibrillar components and form clusters indicative of "Christmas trees" in situ. J. Cell Biol. 157, 743–748.

Koberna, K., Ligasova, A., Malinsky, J., Pliss, A., Siegel, A.J., Cvacková, Z., Fidlerová, H., Masata, M., Fialová, M., Raška, I., Berezney, R., 2005. Electron microscopy of DNA replication in 3-D: evidence for similar-sized replication foci throughout S-phase. J. Cell. Biochem. 94 (1), 126–138.

Křížek, P., Raška, I., Hagen, G.M., 2011. Minimizing detection errors in single molecule localization microscopy. Opt. Express 19, 3226–3235.

Li, J., Santoro, R., Koberna, K., Grummt, I., 2004. The chromatin remodeling complex NoRC controls replication timing of rRNA genes. EMBO J. 24 (1), 120–127.

Little, R.D., Platt, T.H., Schildkraut, C.L., 1993. Initiation and termination of DNA replication in human rRNA genes. Mol. Cell. Biol. 13 (10), 6600–6613.

Long, E.O., Dawid, I.B., 1980. Repeated genes in eukaryotes. Annu. Rev. Biochem. 49, 727–764.

Malinský, J., Koberna, K., Bednar, J., Stulik, J., Raška, I., 2002. Searching for active ribosomal genes *in situ*: light microscopy in light of the electron beam. J. Struct. Biol. 140 (1–3), 227–231.

Melčak, I., Risueno, M.C., Raška, I., 1996. Ultrastructural non-isotopic mapping of nucleolar transcription sites in onion protoplasts. J. Struct. Biol. 116 (2), 253–263.

Ochs, R.L., Lischwe, M.A., Spohn, W.H., Busch, H., 1985. Fibrillarin: a new protein of the nucleolus identified by autoimmune sera. Biol. Cell 54 (2), 123–133.

Ovesný, M., Křížek, P., Borkovec, J., Švindrych, Z., Hagen, G.M., 2014. ThunderSTORM: a comprehensive ImageJ plugin for PALM and STORM data analysis and super-resolution imaging. Bioinformatics. http://dx.doi.org/10.1093/bioinformatics/btu202 (Advance access).

Pliss, A., Koberna, K., Vecerová, J., Malínský, J., Masata, M., Fialová, M., Raška, I., Berezney, R., 2005. Spatio-temporal dynamics at rDNA foci: global switching between DNA replication and transcription. J. Cell. Biochem. 94 (3), 554–565.

Puvion-Dutilleul, F., Bachellerie, J.P., Puvion, E., 1991. Nucleolar organization of HeLa cells as studied by in situ hybridization. Chromosoma 100, 395–409.

Raška, I., 2003. Oldies but goldies: searching for Christmas trees within the nucleolar architecture. Trends Cell Biol. 13, 517–525.

Raška, I., Rychter, Z., Smetana, K., 1983a. Fibrillar centers and condensed nucleolar chromatin in resting and stimulated human lymphocytes. Zeitschrift fur mikroskopischanatomische Forschung 97 (1), 15–32.

Raška, I., Armbruster, B.L., Frey, J.R., Smetana, K., 1983b. Analysis of ring-shaped nucleoli in serially sectioned human lymphocytes. Cell Tissue Res. 234 (3), 707–711.

Raška, I., Dundr, M., Koberna, K., Melcak, I., Risueno, M.M., Torok, I., 1995. Does the synthesis of ribosomal RNA take place within nucleolar fibrillar centres or dense fibrillar components? A critical appraisal. J. Struct. Biol. 114, 1–22.

Raška, I., Shaw, P.J., Cmarko, D., 2006a. New insights into nucleolar architecture and activity. Int. Rev. Cytol. 255, 177–235.

Raška, I., Shaw, P.J., Cmarko, D., 2006b. Structure and function of the nucleolus in the spotlight. Curr. Opin. Cell Biol. 18, 325–334.

Reinhart, M., Casas-Delucchi, C.S., Cardoso, M.C., 2013. Spatiotemporal visualization of DNA replication dynamics. Methods Mol. Biol. 1042, 213–225.

Scheer, U., Benavente, R., 1990. Functional and dynamic aspects of the mammalian nucleolus. Bioessays 12, 14–21.

Schermelleh, L., Solovei, I., Zink, D., Cremer, T., 2001. Two-color fluorescence labeling of early and mid-to-late replicating chromatin in living cells. Chromosome Res. 9, 77–80.

Sirri, V., Urcuqui-Inchima, S., Roussel, P., Hernandez-Verdun, D., 2008. Nucleolus: the fascinating nuclear body. Histochem. Cell Biol. 129, 13–31.

Smirnov, E., Cmarko, D., Kováčik, L., Hagen, G.M., Popov, A., Raška, O., Prieto, J.L., Ryabchenko, B., Amim, F., McStay, B., Ravka, I., 2011. Replication timing of pseudo-NORs. J. Struct. Biol. 173 (2), 213–218.

Warner, J.R., 1999. The economics of ribosome biosynthesis in yeast. Trends Biochem. Sci. 24, 437–440.

Yoon, Y., Sanchez, J.A., Brun, C., Huberman, J.A., 1995. Mapping of replication initiation sites in human ribosomal DNA by nascent-strand abundance analysis. Mol. Cell. Biol. 15, 2482–2489.